Journal of Pharmaceutical and Biomedical Analysis 102 (2015) 199–202

Contents lists available at ScienceDirect

Journal of Pharmaceutical and Biomedical Analysis

journal homepage: www.elsevier.com/locate/jpba

Short communication

A direct heating model to overcome the edge effect in microplates

Chun Yat Lau[a], Alifa Afiah Ahmad Zahidi[a], Oi Wah Liew[b], Tuck Wah Ng[a,*]

[a] Laboratory for Optics and Applied Mechanics, Department of Mechanical & Aerospace Engineering, Monash University, Clayton, Victoria 3800, Australia
[b] Cardiovascular Research Institute, Yong Loo Lin School of Medicine, National University of Singapore, National University Health System, Centre for Translational Medicine, 14 Medical Drive, Singapore 117599, Singapore

ARTICLE INFO

Article history:
Received 7 August 2014
Received in revised form
10 September 2014
Accepted 13 September 2014
Available online 22 September 2014

Keywords:
Edge effect
Finite element
Heating
Microplate
Transparency

ABSTRACT

Array-based tests in a microplate format are complicated by the regional variation in results of the outer against the inner wells of the plate. Analysis of the evaporation mechanics of sessile drops showed that evaporation rate increase with temperature was due to changes in the heat of vaporization, density and diffusion coefficient. In simulations of direct bottom heating of standard microplates, considerable heat transfer via conduction from the side walls was found to be responsible for lower temperatures in the liquid in wells close to the edge. Applying a two temperature heating mode, 304 K at the side compared to 310 K at the bottom, allowed for a more uniform temperature distribution. Transparency microplates were found to inherently possess immunity to the edge effect problem due to the presence of air between the liquid and solid wall.

1. Introduction

In the biochemical laboratory, microplates (or microtiter plates) remain as arguably the most ubiquitous tools in analyte handling for analytical research and clinical diagnostic screening. Keeping the format of analyte handling implements to follow that of standard microplates in developing biochemical analysis instrumentation has the advantage of ready usage with existing readers, thus eliminating the costs associated with developing new readers. It also offers practitioners with familiarity in employing a widely established format. Such a strategy has been harnessed to address various biochemical related needs [1–3] despite the advent of lab-on-a-chip alternatives [4]. Some developments in analyte handling itself to function in this vein have been reported in the context of small volumes [5,6]. More recently, we have advanced the ability to use transparencies, normally applied in conjunction with overhead projectors, in microplate instrumentation [7,8]. The immense cost effectiveness here offers the possibility of application even in resource-limited laboratories.

The scale of testing required in modern biochemical analysis has driven the introduction of multiplexed formats using microplates [9,10]. Multiplex testing, however, presents analytical and quality control challenges. Among the controls that have been introduced include the use of blank areas, positive controls, negative controls, normalization controls, controls for nonspecific binding and to confirm sample addition, cross-reactivity controls, and controls to assess the activity of assay reagents such as the detection conjugate [11]. A factor that continues to complicate array-based tests in a microplate format is the regional variation in results of the outer against the inner wells of the plate, which is often described as the edge effect. The main culprit for this is widely believed to be the zonal differences in the rate of evaporation from the wells [12,13]. Quite naturally, the use of plate seals [14] and tight closures [15] has been advanced to ameliorate the evaporation variation effect. A major cause of evaporation during microplate incubation is temperature. While the effect from temperature gradients have been alluded to [16], there have been no known studies made or approaches advanced to remedy the edge effect through reducing temperature gradients in microplates. Here, we investigate this aspect by providing an analytical link between temperature and evaporation rate, and conducting thermal simulation studies using finite elements (FEM).

2. Analysis of evaporation

Let us consider the evaporation mechanics involved for liquid residing in a standard microplate well (Fig. 1a) and in a transparency microplate well that operates under reduced evaporation [17] (Fig. 1b). Essentially, the latter is a sessile drop in which efforts to characterize its evaporation have been attempted [18]

* Corresponding author. Tel.: +61 3 99054647.
E-mail address: engngtw@gmail.com (T.W. Ng).

http://dx.doi.org/10.1016/j.jpba.2014.09.021
0731-7085/

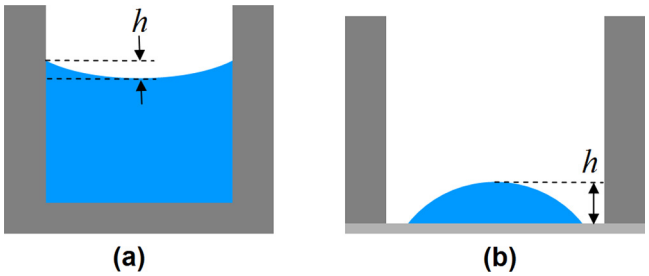

Fig. 1. Schematic depiction of liquid residence in (a) a standard microplate well, and (b) transparency microplate well.

by considering the adjacent air being saturated with vapor due to the rapid interchange of molecules between the liquid and vapor phases. The vapor phase is essentially then a thin saturated region that diffuses outward into the surrounding unsaturated air. Assuming a quasi-equilibrium process for slow evaporation in still air, the evaporation rate of the vapor Q can be taken to be represented by Fick's law such that

$$Q = \rho\frac{dV}{dt} = 4\pi Dr(C_s - C_\infty)f(\theta) \quad (1)$$

where D is the vapor diffusivity in still air, r = radius of air–liquid surface curvature, ρ = density of the liquid, C_s = the saturated vapor concentration at drop surface, C_∞ = the ambient vapor concentration determined by the relative humidity, and $f(\theta)$ = the dependence of evaporation rate on the contact angle. Various factors can affect the evaporation process [19,20], albeit if we consider only a situation in time, Eq. (1) can be simplified to

$$\frac{dV}{dt} = -\frac{2\pi DhM}{\rho RT}(P_s - P_\infty) \quad (2)$$

where h = the height of drop, R = gas constant, M = molecular weight of the liquid, T = temperature in Kelvins of the liquid, P_s = the vapor pressure on the liquid surface, P_∞ = the vapor pressure an infinite distance away (which can be assumed to be zero). P_s is related to T using the Classius–Clayperon relation

$$P_s = \exp\left(\frac{-\Delta H_V}{RT} + K\right) \quad (3)$$

where ΔH_V is the heat of vaporization of the liquid, and K is the value for $\ln(P_s)$ when $\Delta H_V = 0$. Hence Eq. (2) can be rewritten as

$$\frac{1}{h}\frac{dV}{dt} = -\left[\frac{2\pi DM}{\rho RT} exp\left(\frac{-\Delta H_V}{RT} + K\right)\right] \quad (4)$$

We can assume this to be the same in the case of liquid in standard microplate wells.

3. Simulation details

The simulations were conducted using ABAQUS FEA (Dassault Systemes). For the standard microplate, its overall size was 127.76 mm length, 85.48 mm wide, and 14.7 mm high, with the wells kept at a pitch of 9 mm from each other and having diameter and height of 6.5 mm and 11.45 mm respectively. The solid material used throughout was acrylic, while the liquid used was water. In the case of transparency microplates, the transparency thickness was kept at 0.11 mm and the liquid droplets kept at 40 μL volume with a diameter of 5.34 mm in contact with the transparency. The microplate section and the water section were meshed with tetrahedron elements due to their regular shapes, while the transparency section was meshed with rectangular element to achieve an even mesh. The microplate sections in standard microplate model and transparency microplate model have about 720,000 nodes and 650,000 nodes respectively. The transparency sheet has approximately 58,000 nodes and each droplet has about 1500 nodes in the transparency microplate model. The number of nodes in the water section in each well varies from 450 to 3300 depending on the filling ratio. All nodes in both models are approximately 1 mm apart. In the simulations, the boundary elements not affected by heating were fixed at 298 K (which corresponds to typical ambient temperature). The boundary elements subject to direct heating were set at 311 K (to correspond to the body incubation temperatures typically used in biochemical and immunoassays when heating is required). The presence of strong temperature gradients within the liquid body will lead to convection flows that facilitate mass transfer. In our simulations we do not include this effect as our purpose is to establish the average temperature of the liquid in each well.

4. Results and discussion

We start by considering the relationship between temperature and evaporation rate. Eq. (4) appears to portray an anomalous situation that the rate of evaporation is inversely proportional to temperature. In reality, however, only certain parameters in the equation are invariant with temperature, i.e. for water $M = 0.018\,kg\,mol^{-1}$, $R = 8.314\,J\,K^{-1}\,mol^{-1}$, $K = 740.2943$ Pa. At $T = 298$ K (25 °C), $\rho = 997.15\,kg\,m^{-3}$, $\Delta H_V = 1814 \times 10^3\,J\,kg^{-1}$, $D = 25.28 \times 10^{-6}\,m^2\,s^{-1}$; while at $T = 311$ K (38 °C), $\rho = 992.97\,kg\,m^{-3}$, $\Delta H_V = 1891 \times 10^3\,J\,kg^{-1}$, $D = 27.17 \times 10^{-6}\,m^2\,s^{-1}$. Consequently, if we compute the right hand side of Eq. (4), we have values of $-3.91 \times 10^{-9}\,m^2\,s^{-1}$ and $-9.23 \times 10^{-9}\,m^2\,s^{-1}$ for temperatures of 25 °C and 38 °C respectively. This indicates that when the temperature is higher, the evaporation rate increases correspondingly. Hence, this confirms that the key to eliminating the edge effect will be to maintain a constant temperature of the liquid dispensed in all wells.

Fig. 2(a) presents the result of the FEM simulation with a standard microplate well in which only the bottom was heated. It can be seen that there is a considerable heat transfer via conduction from the side walls, causing the liquid in wells close to the edge to experience lower temperatures. Fig. 3(a) present plots of the average liquid temperature sampled at the center and corner wells of a standard microplate at different liquid filling ratios (height of liquid/height of well). The temperature difference trends evident confirm the edge effect through the influence of heat conduction. It can be seen that the temperature in the liquid is generally higher when the liquid filling ratio is increased. This is due to the thermal inertia offered by the liquid body.

In order to overcome the imbalance due to heat conductions, we have simulated the case where the side walls were heated as well as the bottom at the same temperature. As shown in Fig. 2(b), this cursorily portends the capacity to ameliorate the edge effect. On evaluating the average liquid temperature sampled at the center and corner wells of a standard microplate at different liquid filling ratios however (Fig. 3(b)), it can be seen that a reversed effect is attained, i.e. the temperature of the edge wells were higher than the center wells. This is expected due to the contribution of heat from the side walls having a greater influence on the average temperature. Logically, a remedy will be to lower the temperature of the side walls relative to the bottom in order to counteract this imbalance. Fig. 3(c) presents the case where a satisfactory outcome is achieved by keeping the temperature of the side walls at 304 K compared to 310 K at the bottom. It should be noted that different combinations will be needed if the ambient temperature is different.

The need to maintain a dual temperature heating mode can be a challenge in terms of instrumentation development. Since the heat loss due to conductivity is the main culprit for the temperature disparity, a remedy may be to use a material with very low thermal